

# A NON-QUASI-STATIC MODEL OF GAINP/ALGAAS HBT FOR POWER APPLICATIONS

J.Ph. Fraysse\*, D. Floriot\*\*, Ph. Auxémery\*\*\*, M. Campovecchio\*, R. Quéré\*, J. Obregon\*

\*IRCOM CNRS UMR n°6615 Université de Limoges, IUT 7 rue Jules Vallés 19100 BRIVE (FRANCE)

\*\*THOMSON-CSF LCR domaine de Corbeville, route départementale 128, 91401 ORSAY cedex (FRANCE)

\*\*\*ums domaine de Corbeville, route départementale 128, 91401 ORSAY cedex (FRANCE)

## ABSTRACT

A NonLinear (NL) model of HBT obtained from I(V) and S-parameters pulsed measurements is presented. Besides thermal effects, this model includes also two transcapacitances to take into account the Non-Quasi-Static (NQS) effects. It is shown that contrary to a Quasi-Static (QS) one, this model allows to predict accurately the behavior of the device in the whole power range as well as a broad frequency band.

## I - INTRODUCTION

HBTs are promising devices for their power handling capabilities [1] due to the high breakdown voltage  $B_{vcb_0}$  (typically  $B_{vcb_0} > 25V$ ) and the high collector current density drive capabilities. So, it represents a good candidate for power applications. However an efficient design of power amplifiers requires the use of accurate models that are able to predict the behavior of the device in all the bias conditions and in large signal operation.

During the last years a number of models has been proposed [2][3][4][5][6] which deal with various features of the HBT behavior. Some of them take into account NQS effects, but there is no clear evidence of the influence of these effects on power transfer characteristics of the devices. In the present paper, a model is presented in order to take account thermal effects. Moreover the influence of NQS effects is shown by comparison of the large signal simulation results with measured data obtained through frequency. Waveform characterization has been recognized as a valuable tool for the modeling of HBT [7]. In our approach the NQS model has been validated through wave forms measurements at 8 GHz.

## II - MODEL DESCRIPTION

In the classical Quasi-Static (QS) model of fig-1, diffusion capacitances are obtained from a charge

control analysis of the quasi-neutral base region assuming an instantaneous distribution of charges in this region. This leads to define currents in Base Emitter and Base Collector capacitances which are  $i_{BE} = C_{BED}(V_{BE}, V_{BC}) \frac{dV_{BE}}{dt}$ ,  $i_{BC} = C_{BCD}(V_{BE}, V_{BC}) \frac{dV_{BC}}{dt}$ . The delay time  $\tau_d$  and the capacitances  $C_{BED}$ ,  $C_{CED}$  and  $C_{BCD}$  can be obtained from small signal multibias [S] parameters measurements using the simple formula of eq-1.

$$\begin{aligned} C_{BED} &= \frac{\text{Im}(Y_{11} + Y_{12})}{\omega} & C_{CED} &= \frac{\text{Im}(Y_{22} + Y_{12})}{\omega} \\ C_{BCD} &= -\frac{\text{Im}(Y_{12})}{\omega} & \tau_d &= -\frac{1}{\omega} \frac{\text{Im}(Y_{21} - Y_{12})}{\text{Re}(Y_{21} - Y_{12})} \end{aligned} \quad (1)$$

Those equations allow a very good fit of S parameters data in the active region of the device when the BC junction is turned off. However in the saturation region these formula give negative values for the output capacitance  $C_{CED}$  and the delay  $\tau_d$ . This can be seen from fig-4 where the variation of reactive elements extracted from S parameters measurements versus  $V_{CE}$  at constant  $I_B$  are plotted.

Some authors have pointed out the fact that QS models do not predict correctly the high frequency performances of Bipolar transistors [8] and suggest the use of transcapacitances. Those ones allow to take into account the charge distribution time in the quasi-neutral base [9]. We have adopted this approach here and intrinsic part of the NL model fig-1 is modified as shown in fig-2. In this model a transcapacitance  $C_{BEc}$  has been added between the Base and Emitter nodes, while the delay  $\tau$  in the collector current source has been removed and replaced by the transcapacitance  $C_{BCe}$ . The Y parameters of fig-2 are given below:

$$\begin{aligned} Y_{11} &= g_{BC} + g_{BE} + j\omega(C_{BE} + C_{BC} + C_{BCe} + C_{BEc}) \\ Y_{12} &= -g_{BC} - j\omega(C_{BC} + C_{BEc}) \\ Y_{21} &= -g_{BC} + g_m - j\omega(C_{BC} + C_{BCe}) \\ Y_{22} &= g_{BC} + g_d + j\omega(C_{BC}) \end{aligned} \quad (2)$$

These values can be related to the previous values of the equivalent circuit of fig-1 by :

$$\begin{aligned} C_{BEd} &= C_{BE} + C_{BCE} \\ C_{BCd} &= C_{BC} + C_{BEC} \\ C_{CED} &= -C_{BEC} \\ \tau_d &= \frac{C_{BCE} - C_{BEC}}{gm} \end{aligned} \quad (3)$$

Inspection of eq-3 allows us to explain the negative values of the extracted  $C_{CED}$  and  $\tau_d$  using classical circuit in the saturation region. Indeed, in this region,  $C_{BEC}$  reflects the charge redistribution time in the base when the charges are injected from the collector region, which is the case when the Base Collector junction is forward biased. Moreover, the capacitance  $C_{BEC}$  allows to account for Kirk effect.

### III - MODEL EQUATIONS

From the topology shown in fig-2, all the elements of the equivalent circuit have been determined from pulsed  $I(V)$  and pulsed  $[S]$  parameters measurements [10] at various temperatures. The temperature dependence of the elements has been taken into account and the temperature is calculated through the electrical equivalent circuit ( $R_{th}$ ,  $C_{th}$ ) of fig-1. The equations of current sources, the temperature dependence of parameters and the value of the thermal resistance has been determined in [11].

Equations for capacitances and transcapacitances are given below.

$$\begin{aligned} C_{BE} &= \frac{C_{jE0}}{\sqrt{1 - \frac{V_{BE}}{\phi_{BE}}}} + (1 - \alpha) \cdot C_{dE} \\ C_{BCE} &= \alpha \cdot C_{dE} \\ C_{dE} &= C_{dE0}(T) \cdot \exp\left(\frac{q \cdot V_{BE}}{Nt \cdot K \cdot T}\right) \\ C_{BC} &= C_{BC0} + C_{BC1} \exp(V_{BC} \cdot a) \\ C_{BEC} &= C_{BEC0} \cdot \exp(V_{BC} \cdot b) \end{aligned} \quad (4)$$

Charge associated with these capacitances have been introduced in the HP EESOF LIBRA Non Linear simulator.

The transistor we used for this modeling was a GaInP/AlGaAs HBT with four emitter fingers of  $2 \times 30 \mu\text{m}^2$  of the Thomson LCR foundry. The transistor was ballasted for thermal stability and has a thermal shunt. The thermal resistance  $R_{th}$  obtained from pulsed measurements was  $159^\circ\text{C}/\text{W}$ . The temperature dependence of the base emitter turn on

voltage was  $-1.4\text{mV}/^\circ\text{C}$ . For this transistor the values of the capacitances parameters are as follows :

$$\alpha=0.33, a=0.85; b=5; C_{BC0}=100\text{fF}; C_{BC1}=39\text{fF}; C_{BEC0}=0.01\text{fF}.$$

Using these values, the  $[S]$  parameters are well fitted in multibias conditions.

### IV - LARGE SIGNAL BEHAVIOR

In order to validate the proposed model, extensive frequency and time domain load-pull have been performed for maximum power added or maximum power-added efficiency load conditions. In fig-3 frequency load pull measurements at 6 GHz, 10 GHz and 15 GHz are presented together with the simulation results. It can be seen that a very good fit has been obtained between measurements (points) and simulation (full line) at the three frequencies, both for power gain and collector average current. In order to investigate the effects of the NQS effects we have performed the same simulation with the classical model (dotted line). It can be seen that there is a good agreement between the two models as far as the load line enters in the saturation region. Then the collector current exhibits a saturation phenomena that has never been observed or measured.

More investigations have been performed on the large signal behavior of the device using a time-domain vectorial nonlinear network analyser [12]. The fundamental frequency was chosen to be 8.1 GHz and the first three harmonics were measured with this system. All these harmonics have a  $50 \Omega$  load. The input power was set to 29.7 mW with an average Collector current of 68 mA. The comparison of time domain waveforms shown in fig-5 demonstrates the ability of the NL model to accurately describes the large signal behavior of the HBT.

### V - CONCLUSION

A NQS model of GaInP/AlGaAs HBT has been developed and successfully compared to extensive load-pull measurement data. The model based on pulsed measurements results takes into account the temperature and can be used with accuracy beyond 20 GHz. Moreover this model has been validated with time domain and load-pull measurements.

### ACKNOWLEDGMENT

The authors would like to thank Thomson TCM for the financial support of J.Ph Fraysse's thesis and J.P. Viaud for helpful discussions.

## REFERENCES

[1] **S.L. Delage and al:** "Power GaInP/GaAs HBT MMICs" EuMC Cannes 94, Vol 2, pp 1143-1148.

[2] **P. Chris Grossman, John Choma:** "Large Signal Modeling of HBT's Including Self-Heating and Transit Time Effects" IEEE Trans. MTT, vol 40, n°3, pp 449-464, March 1992.

[3] **Michael Y. Frankel, Dimitris Pavlidis:** "An Analysis of the large-Signal Characteristics of AlGaAs/GaAs Heterojunction Bipolar Transistors" IEEE Trans. MTT, vol 40, n°3, pp 465-474, March 1992.

[4] **Douglas A. Teeter and al:** "Large-Signal HBT Characterization and Modeling at Millimeter Wave Frequencies" IEEE Trans. MTT, vol 41, n°6/7, pp 1087-1093, June/July 1993.

[5] **Ke Lu, Thomas J. Brazil:** "A New Spice-Type Heterojunction Bipolar Transistor Model For DC, Microwave Small-Signal Circuit Simulation" IEEE MTT-S Digest 94, San-Diego, TH3B-5, pp 1579-1582.

[6] **Robert Anholt:** "Electrical and Thermal Characterization of MESFETs, HEMTs, and HBTs" Artech House, Boston.London, 1995.

[7] **Ce-Jun Wei and al:** " Waveform-Based Modeling and Characterization of Microwave Power Heterojunction Bipolar Transistor" IEEE Trans. MTT, vol 43, n°12, Dec 1995.

[8] **Jerry G. Fossum, Surya Veeraraghavan:** "Partitioned- Charge-Based Modeling of Bipolar Transistors for Non-Quasi-Static Circuit Simulation" IEEE Trans. EDL, vol. 7, n°12, pp 652-654, Dec.1986.

[9] **Helmut Klose, Armin W. Wieder:** "The Transient Integral Charge Control Relation — A Novel Formulation of the Currents in a Bipolar Transistor" IEEE Trans. ED, vol 34, n°5, pp 1090-1099, May 1987.

[10] **J.P. Viaud and al:** "Nonlinear RF Characterization and Modeling of Heterojunction Bipolar Transistors under Pulsed Conditions" EMC Proceedings, vol 2, pp 1610-1615, sep 1994.

[11] **T. Peyretaille and al:** "A Pulsed-Measurement Based Electrothermal Model of HBT with Thermal Stability Prediction Capabilities" IEEE MTT-S 97, Denver, OF2-7.

[12] **J.M. Nebus and al:** "Optimisation of power added efficiency of transistors using the combinacion of an active harmonic load-pull setup with a broadband vectorial nonlinear network analyzer" IEEE MTT-S 96, Workshop, San-Francisco, TH2 B3, pp 1365-1368.

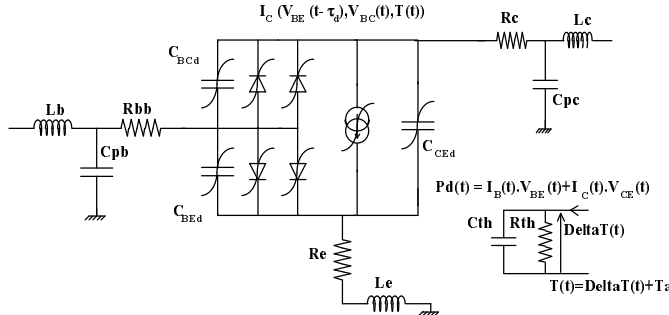


fig-1: Nonlinear HBT equivalent circuit

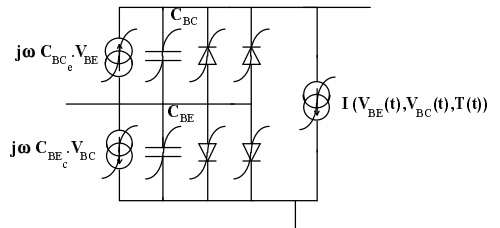


fig-2: Intrinsic NQS device of HBT

◆ X + Measurements at 6, 10 and 15 GHz — simulations with NQS model - - - simulations with QS model

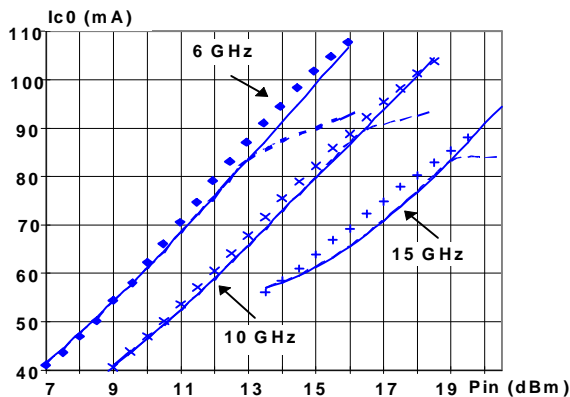


fig-3a: Simulated collector average current compared with load-pull measurements ( $V_{CEO}=8V$ )

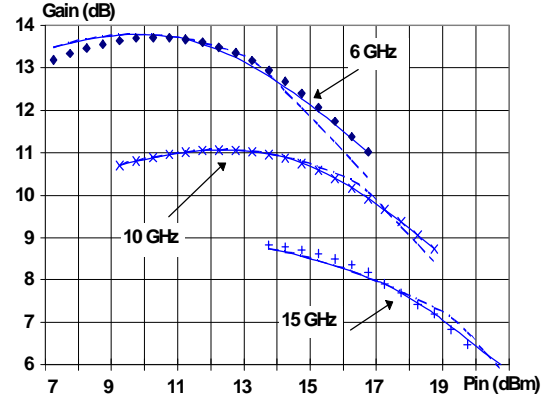


fig-3b: Simulated power gain compared with load-pull measurements ( $V_{CEO}=8V$ )

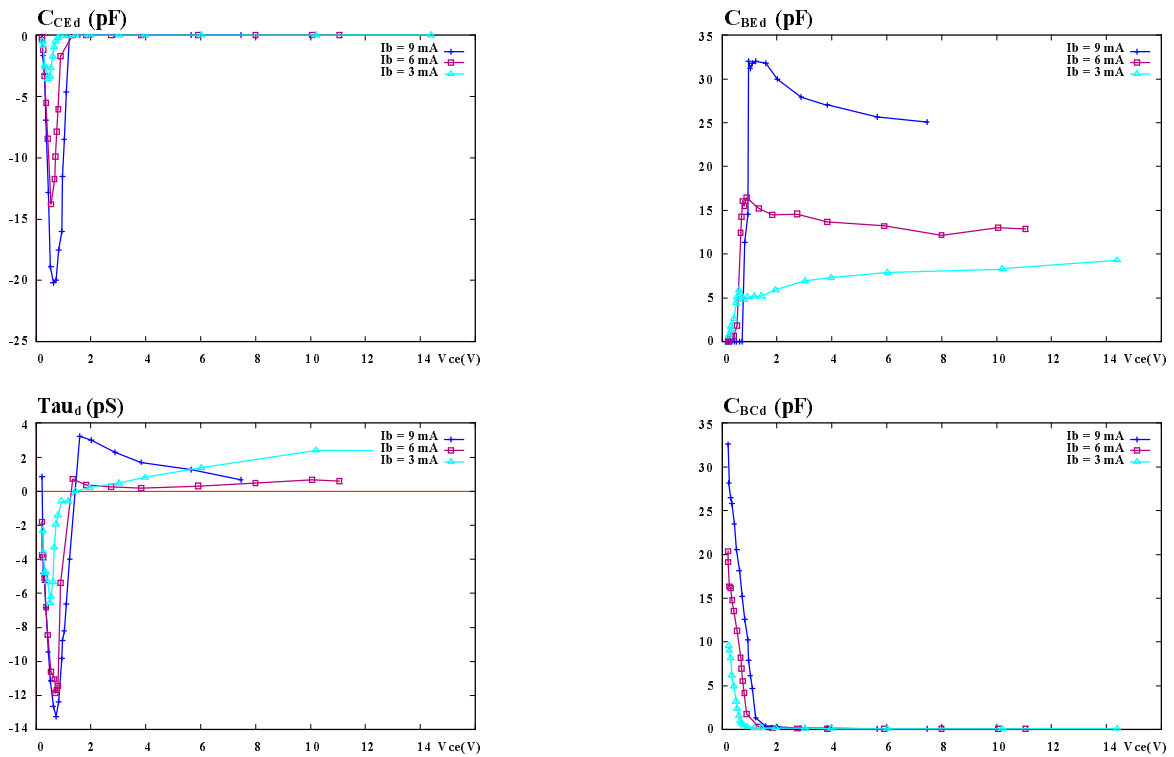


fig-4: reactive elements extracted from S-parameters of a  $4 \times 2 \times 30 \mu\text{m}^2$  GaInP/GaAs HBT

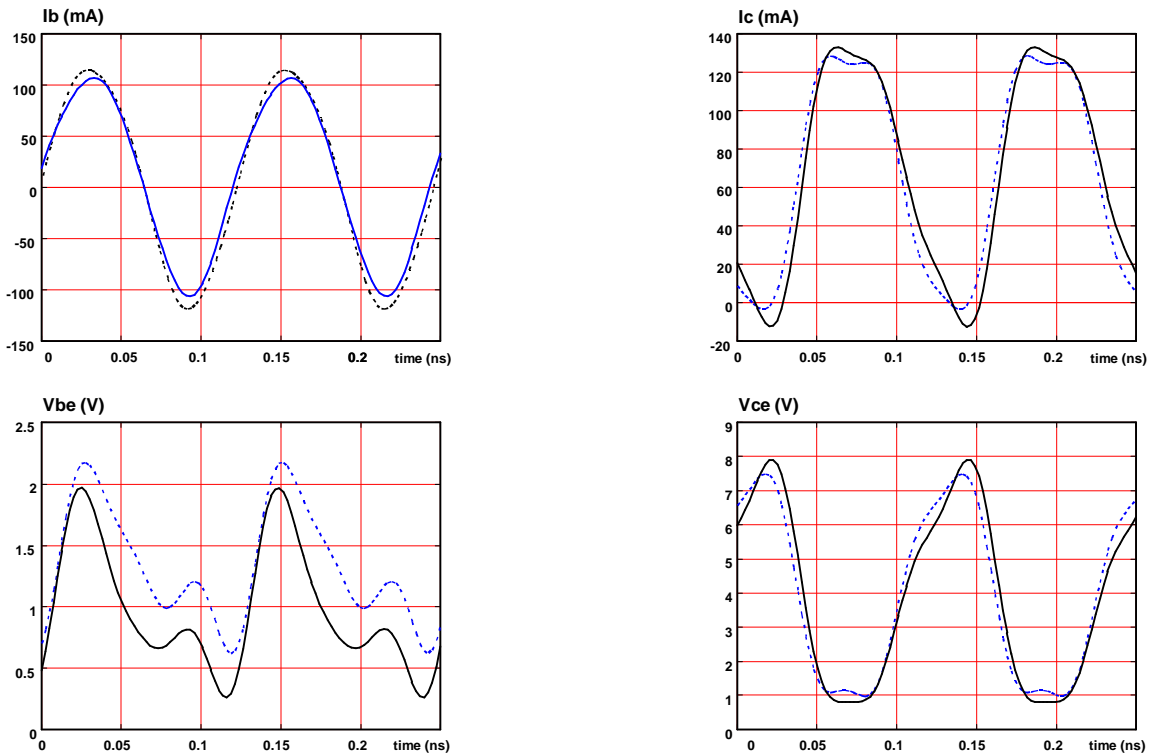


fig-5 Extrinsic voltage and current waveforms at the base and collector  
 (----) Simulations (—) Measurements ( $V_{CE0}=4\text{V}$ ,  $I_{C0}=68\text{ mA}$ ,  $P_{in}=29.7\text{ mW}$ )